ISSN 1674-1056
http://cpb.iphy.ac.cn
http://iopscience.iop.org/cpb
中国物理 B
Chinese Physics
中国物理 Chinese Physics B

Propagation of acoustic waves in a fluid-filled pipe with periodic elastic Helmholtz resonators

Dian-Long Yu(郁殿龙), Hui-Jie Shen(沈惠杰), Jiang-Wei Liu(刘江伟), Jian-Fei Yin(尹剑飞), Zhen-Fang Zhang(张振方), Ji-Hong Wen(温激鸿)
Citation: Chin. Phys. B . 2018, 27(6): 064301. **doi:** 10.1088/1674-1056/27/6/064301

Journal homepage: http://cpb.iphy.ac.cn; http://iopscience.iop.org/cpb

What follows is a list of articles you may be interested in

Membrane-based acoustic metamaterial with near-zero refractive index

Yi-Feng Li(李义丰), Jun Lan(蓝君), Hui-Yang Yu(余辉洋), Xiao-Zhou Liu(刘晓宙), Jia-Shu Zhang(张嘉澍)
Chin. Phys. B . 2017, 26(1): 014302. **doi:** 10.1088/1674-1056/26/1/014302

Low band gap frequencies and multiplexing properties in 1D and 2D mass spring structures

Arafa H Aly, Ahmed Mehaney
Chin. Phys. B . 2016, 25(11): 114301. **doi:** 10.1088/1674-1056/25/11/114301

Wave propagation in beams with anti-symmetric piezoelectric shunting arrays

Sheng-Bing Chen(陈圣兵), Gang Wang(王刚)
Chin. Phys. B . 2016, 25(3): 034301. **doi:** 10.1088/1674-1056/25/3/034301

Mechanical properties of $Ga_xIn_{1-x}As_yP_{1-y}$/GaAs systemat different temperatures and pressures

A. R. Degheidy, E. B. Elkenany
Chin. Phys. B . 2015, 24(9): 094302. **doi:** 10.1088/1674-1056/24/9/094302

Acoustic scattering from a submerged cylindrical shell coated with locally resonant acoustic metamaterials

Li Li, Wen Ji-Hong, Cai Li, Zhao Hong-Gang, Wen Xi-Sen
Chin. Phys. B . 2013, 22(1): 014301. **doi:** 10.1088/1674-1056/22/1/014301

Propagation of acoustic waves in a fluid-filled pipe with periodic elastic Helmholtz resonators*

Dian-Long Yu(郁殿龙)[1,†], Hui-Jie Shen(沈惠杰)[2], Jiang-Wei Liu(刘江伟)[1], Jian-Fei Yin(尹剑飞), Zhen-Fang Zhang(张振方)[1], and Ji-Hong Wen(温激鸿)[1]

[1] *Laboratory of Science and Technology on Integrated Logistics Support, National University of Defense Technology, Changsha* 410073, *China*
[2] *College of Power Engineering, Naval University of Engineering, Wuhan* 430033, *China*

(Received 1 January 2018; revised manuscript received 27 March 2018; published online 10 May 2018)

Helmholtz resonators are widely used to reduce noise in a fluid-filled pipe system. It is a challenge to obtain low-frequency and broadband attenuation with a small sized cavity. In this paper, the propagation of acoustic waves in a fluid-filled pipe system with periodic elastic Helmholtz resonators is studied theoretically. The resonance frequency and sound transmission loss of one unit are analyzed to validate the correctness of simplified acoustic impedance. The band structure of infinite periodic cells and sound transmission loss of finite periodic cells are calculated by the transfer matrix method and finite element software. The effects of several parameters on band gap and sound transmission loss are probed. Further, the negative bulk modulus of periodic cells with elastic Helmholtz resonators is analyzed. Numerical results show that the acoustic propagation properties in the periodic pipe, such as low frequency, broadband sound transmission, can be improved.

Keywords: acoustic metamaterial, band gap, sound transmission loss, elastic Helmholtz resonator, noise control

PACS: 43.40.+s, 47.35.Lf, 62.60.+v **DOI:** 10.1088/1674-1056/27/6/064301

1. Introduction

Piping systems with fluid loading are frequently encountered in engineering, such as in heat exchanger tubes, main steam pipes, and hot/cold leg pipes in nuclear steam supply systems, oil pipelines, pump discharge lines, marine risers, etc.[1,2] The vibration and noise in a piping system can affect the precision of the system control and the normal work functions of downstream equipment.[3] Fortunately, this noise can be sufficiently reduced to a level of the noise from other automotive sources, or even lower, by means of a well-designed muffler (also called a silencer).[4] However, a limitation exists in conventional mufflers, namely, their ability to attenuate low-frequency noise.[2] Therefore, the control of low-frequency noise transmission in the pipe is an important and challenging problem.

A Helmholtz resonator (HR) is often used to reduce noise in a narrow frequency band. This type of resonator has a high transmission loss in a narrow band at its resonance frequency.[5] It is easy to design this resonator to have a desired low frequency with a larger sized cavity because the resonance frequency is determined by the geometric ratio of the cavity to its neck.

The effect of wall elasticity on the resonance frequency of an HR has received considerable attention.[6–9] The results indicate that the wall compliance will reduce the resonance frequency in comparison with an identically shaped rigid cavity. Additionally, sound transmission loss (STL) of an HR in a fluid-filled piping system has been investigated.[3,10] However, for wide frequency band noise control, there is more work that needs to be done. It is a challenge to obtain a low-frequency and broadband gap with a small sized HR in the fluid-filled piping system.

Recently, artificially designed periodic acoustic materials/structures, referred to as phononic crystals or acoustic metamaterials, have emerged. The acoustic wave propagation in phononic crystals or acoustic metamaterials can be strongly modulated, which provides a possible way to solve the problems of vibration and noise control.[11–13] Novel phenomena, such as band gap[14] negative effective physical characteristics,[15] acoustic cloaking,[16] extraordinary sound absorption,[17,18] and sub-wavelength imaging,[19] have been theoretically proven or experimentally observed.

By introducing repeated shunted rigid HRs, the propagation of acoustic waves in a pipe is analyzed.[2,20–22] To the best of our knowledge, in the available literature, the propagation of acoustic waves in a fluid-filled pipe system with periodic HRs was studied but the elastic pipe walls have not been taken into consideration.

In this paper, the propagation of acoustic waves in a pipe with periodic elastic Helmholtz resonators is studied. The effects of several parameters on the band gaps and sound transmission loss are also investigated.

*Project supported by the National Natural Science Foundation of China (Grant Nos. 11372346, 51405502, and 51705529).
†Corresponding author. E-mail: dianlongyu@vip.sina.com
© 2018 Chinese Physical Society and IOP Publishing Ltd

2. Model and governing equations

2.1. Acoustic impedance and resonance frequency of an elastic HR

An HR with an elastic wall is presented in Fig. 1, where l_n and D_n are the length and the diameter of the neck, respectively; l_c and D_c are the length and the diameter of the cavity, respectively; L and D are the length and the diameter of the pipe, respectively; and d is the thickness of the elastic wall. The cavity with an elastic wall is composed of three parts: the top panel, the cylinder, and the bottom panel. The cavity and pipe are filled with fluid, settled as the shadowed regions in Fig. 1.

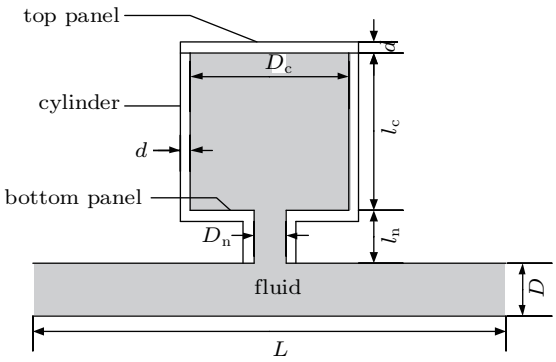


Fig. 1. Sketch of an elastic HR.

For the HR with a rigid wall, the acoustic impedance can be expressed as[2,9,21]

$$Z_H = \mathrm{i}\left(\omega M_{ha} - \frac{1}{\omega C_{ha}}\right), \tag{1}$$

where the acoustic mass $M_{ha} = \rho_0 l_e / S_n$ and the acoustic capacitance $C_{ha} = V_c/\rho_0 c_0^2$, and ρ_0 and c_0 are the density and velocity of the fluid, $S_n = \pi D_n^2/4$ is the cross-sectional area of the neck, $V_c = \pi D_c^2 l_c/4$ is the volume of the resonance cavity, and $l_e = l_n + \delta_c + \delta_p$ is the effective length of the neck, δ_c and δ_p are the acoustic length correction factors corresponding to the cavity volume and main duct interfaces, respectively, ω is the angular frequency, and $\mathrm{i}^2 = -1$.

Based on plane wave theory, the resonance frequency can be expressed using the low-frequency approximation as $f_H = (c_0/2\pi)\sqrt{S_n/V_c l_e}$.

For an HR with an elastic wall, if the acoustic impedances of the cylinder and the bottom panel are neglected, the acoustic impedance of an elastic HR can be expressed as[9]

$$Z_{EH} = \mathrm{i}\omega M_{ha} + \frac{1}{\mathrm{i}\omega\left(C_{ha} + \dfrac{C_1}{1-\omega^2 M_1 C_1}\right)}, \tag{2}$$

where $M_1 = 72d\rho/5\pi D_c^2$ and $C_1 = \pi D_c^6\left(1-\sigma^2\right)/1024Ed^3$ are the acoustic mass and the acoustic capacitance of the top panel, respectively, while ρ, E, and σ are the density, Young's modulus, and Poisson's ratio of the top panel, respectively.

For a top panel with a clamped boundary condition, the resonance frequency can be given as[9]

$$f_{EH} = \frac{1}{2\pi}\left(\frac{-b \pm \sqrt{b^2 - 4ac}}{2a}\right)^{1/2}, \tag{3}$$

where $a = M_{ha}C_{ha}M_1C_1$, $b = -(M_{ha}C_{ha} + M_{ha}C_1 + M_1C_1)$, and $c = 1$.

2.2. Transfer matrix and dispersion relation of an infinite periodic pipe with elastic HRs

The piping system, consisting of a uniform pipe with HRs attached periodically, is sketched in Fig. 2. The lattice constant is L.

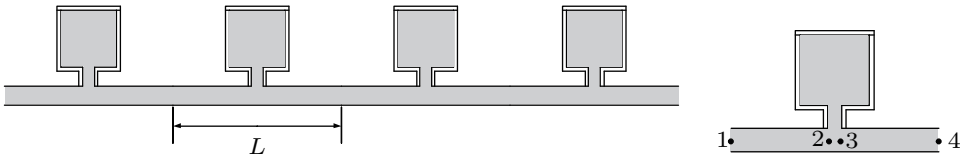


Fig. 2. (a) Sketch of infinite periodic pipe with elastic HRs and (b) single unit.

Acoustic wave propagation in this system can be described under the assumption of a plane wave when we focus on the low-frequency range.

The sound pressure (p) and the volume velocity (u) can be expressed as follows:[4,5,23]

$$p = A\mathrm{e}^{-\mathrm{i}kx} + B\mathrm{e}^{-\mathrm{i}kx}, \tag{4}$$

$$u = \frac{1}{Z_0}\left(A\mathrm{e}^{-\mathrm{i}kx} + B\mathrm{e}^{-\mathrm{i}kx}\right), \tag{5}$$

where A and B are the magnitudes of the incident wave and the reflected wave, and $Z_0 = \rho_0 c_0/S_0$ is the acoustic impedance of the pipe, with $S_0 = \pi D^2/4$ being the cross-sectional area of the pipe, and k is the wave number.

By introducing the state vector

$$\boldsymbol{W}_n = \begin{pmatrix} p \\ u \end{pmatrix},$$

the transfer matrix relation for a uniform pipe section with a length of $L/2$ between point 1 and point 2 in the nth cell is

$$\boldsymbol{W}_n^1 = \boldsymbol{T}_n^1 \boldsymbol{W}_n^2, \tag{6}$$

where

$$\boldsymbol{T}_{\mathrm{n}}^{1}=\begin{bmatrix}\cos(kL/2) & \mathrm{i}Z_0\sin(kL/2)\\ (\mathrm{i}/Z_0)\sin(kL/2) & \cos(kL/2)\end{bmatrix}.$$

Similarly,

$$\boldsymbol{W}_{\mathrm{n}}^{3}=\boldsymbol{T}_{\mathrm{n}}^{2}\boldsymbol{W}_{\mathrm{n+1}}^{1}. \tag{7}$$

For the HR, the transfer matrix between point 2 and point 3 can be obtained using the continuity of the sound pressure and the volume velocity, as follows:[5]

$$\boldsymbol{W}_{\mathrm{n}}^{2}=\boldsymbol{T}_{\mathrm{n}}^{H}\boldsymbol{W}_{\mathrm{n}}^{3}, \tag{8}$$

where

$$\boldsymbol{T}_{\mathrm{n}}^{\mathrm{H}}=\begin{bmatrix}1 & 1\\ M/Z_{\mathrm{EH}} & 1\end{bmatrix},$$

with M denoting the number of HRs in one cell.

Combining Eqs. (6), (7), and (8) yields the following relation between the n-th cell and the $(n+1)$-th cell:

$$\boldsymbol{W}_{\mathrm{n}}^{1}=\boldsymbol{T}\boldsymbol{W}_{\mathrm{n+1}}^{1}, \tag{9}$$

where $\boldsymbol{T}=\boldsymbol{T}_{\mathrm{n}}^{1}\boldsymbol{T}_{\mathrm{n}}^{H}\boldsymbol{T}_{\mathrm{n}}^{2}$ is the transfer matrix.

Due to the periodicity of the infinite structure in the x direction, the vector $\boldsymbol{W}_{\mathrm{n}}$ must satisfy the Bloch theorem, i.e.,[1,2]

$$\boldsymbol{W}_{\mathrm{n}}=\mathrm{e}^{\mathrm{i}qL}\boldsymbol{W}_{n-1}, \tag{10}$$

where q is the Bloch wave vector in the x direction.

Based on Eqs. (9) and (10), the dispersion relation of the model can be obtained as follows:

$$\cos(qL)=\cos(kL)+\frac{\mathrm{i}MZ_0}{2Z_{\mathrm{EH}}}\sin(kL). \tag{11}$$

For a given ω, equation (11) supplies the values of q. Depending on whether q is real or has an imaginary part, the corresponding wave propagates through the beam (pass band) or is damped (band gap).

2.3. Transfer matrix and dispersion relation of finite periodic pipe with elastic HRs

With respect to a finite periodic structure with N unit cells, the transmitting relationship for the state vectors at the inlet and the outlet can be derived as

$$\boldsymbol{T}_N=\boldsymbol{T}^N. \tag{12}$$

The STL can be represented using the transfer matrix as follows:[5]

$$\mathrm{STL}=20\log_{10}\left|\frac{\boldsymbol{T}_N(1,1)+\boldsymbol{T}_N(1,2)/Z_0+\boldsymbol{T}_N(2,1)Z_0+\boldsymbol{T}_N(2,2)}{2}\right|. \tag{13}$$

3. Resonance frequency and STL of pipe with a single cell

The geometry of the pipe-mounted HR considered in the calculation is shown in Fig. 1. The geometric parameters are chosen as follows:[3] $D=0.08$ m, $L=0.6$ m, $l_{\mathrm{c}}=0.2$ m, $D_{\mathrm{c}}=0.16$ m, $d=0.005$ m, $D_{\mathrm{n}}=0.034$ m, and $l_{\mathrm{n}}=0.087$ m. In this case, the effective length of the neck is $l_{\mathrm{e}}=0.1084$ m. The materials of the cylinder and bottom panel are both steel with a density of 7800 kg/m^3, Young's modulus of 2.1×10^{11} Pa, and Poisson's ratio of 0.3; the material of the top panel is epoxy with a density of 1180 kg/m^3, Young's modulus $E=4.35\times10^{9}$ Pa, and Poisson's ratio of $\sigma=0.37$. The fluid in the pipe is water with density $\rho_0=1000$ kg/m^3, and velocity $c_0=1500$ m/s.

First, we consider the number of HRs in a single cell $M=1$.

For a rigid HR, the STL calculated by the transfer matrix method (TMM) is illustrated as the black solid line in Fig. 3. In this case, the resonance frequency is 340 Hz. The STL is also calculated using the finite-element method (FEM) with COMSOL Multiphysics software. In the calculation, the coupling between the structural mechanics module and the acoustics module is considered. The STL calculated using FEM is shown as a black dotted line in Fig. 3, in which the resonance frequency is 335 Hz. It can be found that the results calculated using TMM and FEM agree well with each other for a rigid HR.

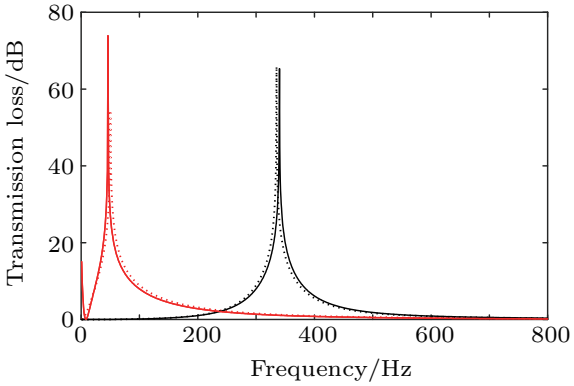


Fig. 3. (color online) STL of a single HR. The black solid and black dotted lines correspond to the STLs of one rigid HR, calculated by TMM and COMSOL, respectively. The red solid and red dotted lines correspond to the STLs of a single elastic HR, calculated by TMM and COMSOL, respectively.

For an elastic HR, the material of the top panel is softer than the materials of the cylinder and bottom panel; this can be simplified into a clamped boundary condition. Based on Eq. (13), the STL calculated by TMM is illustrated as the red solid line in Fig. 3. In this case, the resonance frequency is

46 Hz. The STL calculated using FEM is shown as a red dotted line in Fig. 3, in which the resonance frequency is 50 Hz. The good agreement between TMM and FEM validates the correctness of the simplified acoustic impedance in Eq. (2) and the resonance frequency in Eq. (3).

From Fig. 3, it is observed that the resonance frequency of an elastic HR is much less than that of a rigid HR with the same cavity size. To reveal the mechanism of the low frequency resonance, the sound pressure level of a rigid HR and the displacement deformation of an elastic HR at the resonance frequency are calculated using the FEM, and the results are illustrated in Fig. 4. One can find that a rigid HR generates the acoustic cavity resonance at 335 Hz, and an elastic HR generates the top panel structure resonance at 46 Hz.

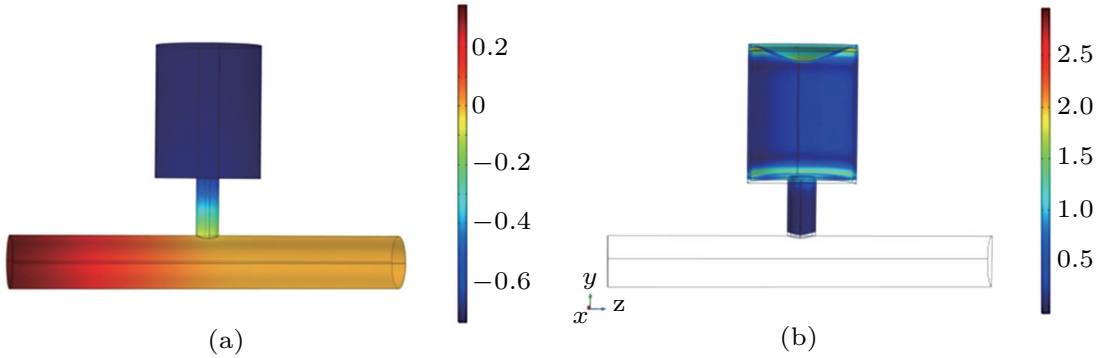


Fig. 4. (color online) (a) Sound pressure level of rigid HR at 335 Hz, (b) displacement deformation of an elastic HR at 46 Hz.

Therefore, the resonant frequency of an elastic HR depends on the top panel but not on the cavity size. Therefore, we can assert that the cavity size will not affect the resonant frequency. The STLs for various lengths of the cavity are illustrated in Fig. 5. The solid, dash dot, and dotted lines correspond to $l_c = 0.2$ m, 0.1 m, and 0.05 m, respectively. The resonant frequencies are almost unchanged for the various cavity sizes, but it is seen that when the cavity length l_c decreases, the STL increases.

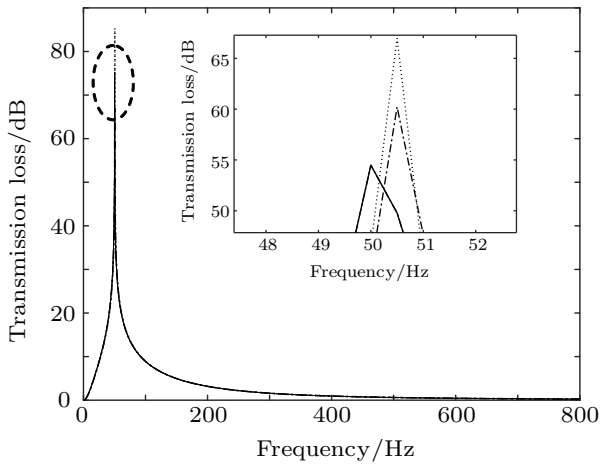


Fig. 5. Frequency-dependent STLs for cavity length $l_c = 0.2$ m (solid line), 0.1 m (dash dot line), and 0.05 m (dotted line).

The effect of the number of HRs, M, in one cell on the STL is considered. In Fig. 6, the STLs for various values of number of HR, M, are calculated. The solid, dash dot and dotted lines correspond to $M = 1$, 2, and 4, respectively. This indicates that the number of HRs in one cell will increase the STL value in a broadband frequency range.

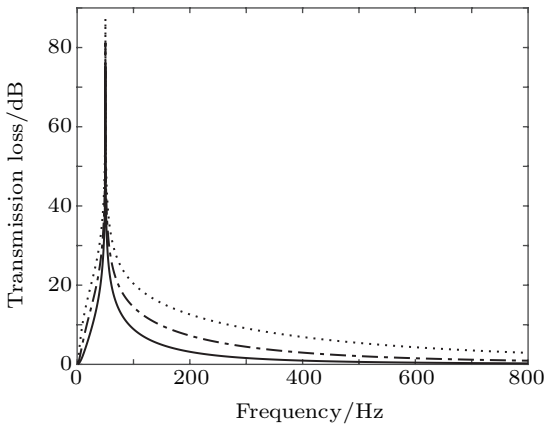


Fig. 6. The STLs for the number of HR, M =1 (solid line), 2 (dash dot line), and 4 (dotted line).

4. Band structure and STL of periodic pipe

For a periodic pipe with elastic HRs, illustrated in Fig. 2(a), the band structure calculated by Eq. (11) is shown as black lines in Fig. 7(a). The elastic parameters and geometric parameters are chosen to be the same as those in Fig. 3. A low-frequency and broadband locally resonant gap generates between 45 Hz and 378 Hz, whose normalized gap width is $\Delta f/f_g = 1.57$, where Δf and f_g are the absolute gap width and the midgap frequency. The band structure is also calculated using COMSOL, which has been successfully used to calculate the band gaps of Phononic Crystals and acoustic metamaterials.[24,25] In the COMSOL calculation, the Floquet periodic conditions are applied to both of the pipe cross sections. The coupling between the structural mechanics module and the acoustics module is considered. The band structure that is calculated using the FEM is shown as a blue dotted line

in Fig. 7(a). It can be found that the results calculated using the TMM and the FEM show good agreement with each other. However, for the FEM results, there is an additional flat band at approximately 611 Hz. As a comparison, the band structure of periodic HRs with rigid walls is illustrated as a black dash dot line, which is calculated by TMM. In this case, the first gap extends from the frequency of 302 Hz to 498 Hz, whose normalized gap width $\Delta f/f_{\rm g} = 0.49$. Therefore, a pipe with periodic elastic HRs will be beneficial to the generation of a low-frequency and broadband gap. The STLs of five periodic cells with elastic walls and rigid walls are calculated and illustrated with black solid and black dash dot lines in Fig. 7(b). The STL that is calculated by the FEM is shown as a blue dotted line.

Furthermore, the eigenvalues of a single unit cell with Floquet periodic conditions are calculated. The first and second non-zero eigenvalues correspond to the points A and C, for which the Bloch wave vector is $q = -\pi/a$, and the eigenvalue corresponds to point B for which $q = 0$. The mode shapes of points A, B, and C are illustrated in Figs. 8(a)–8(c). From points A and B, one can find that the band gap formation mechanism is due to the resonance of the top panel, and that the flat band at point C is due to the second mode of the top panel.

In Fig. 9, the effects of the geometric parameters of an HR on the band gaps are considered, including the length ($l_{\rm n}$), the diameter ($D_{\rm n}$) of the neck, the length ($l_{\rm c}$), and the diameter ($D_{\rm c}$) of the cavity. The solid lines with circular (o) and square (□) symbols describe the start frequency and the cutoff frequency, respectively, of the band gap for the periodic elastic HRs. For comparison, the effect of a rigid HR is also calculated, and the result is illustrated by using a dash–dot line. In each calculation, only one parameter is varied, while all other parameters are kept to be the same as those in Fig. 7. From Fig. 9, we can find that the start frequency and the cutoff frequency are independent of the length of cavity $l_{\rm c}$, which could be an indication that the formation mechanism of the low-frequency band gap is due to the resonance of the top panel but not the HR cavity. Figure 9 also reveals that the start frequency becomes lower as the diameter of the cavity ($D_{\rm c}$) increases, which is due to the resonant frequency becoming lower for the large top panel. However, the cutoff frequency remains unchanged if the diameter of the cavity is large enough. The effects of the geometric parameters of the neck on the start frequency are all trivial.

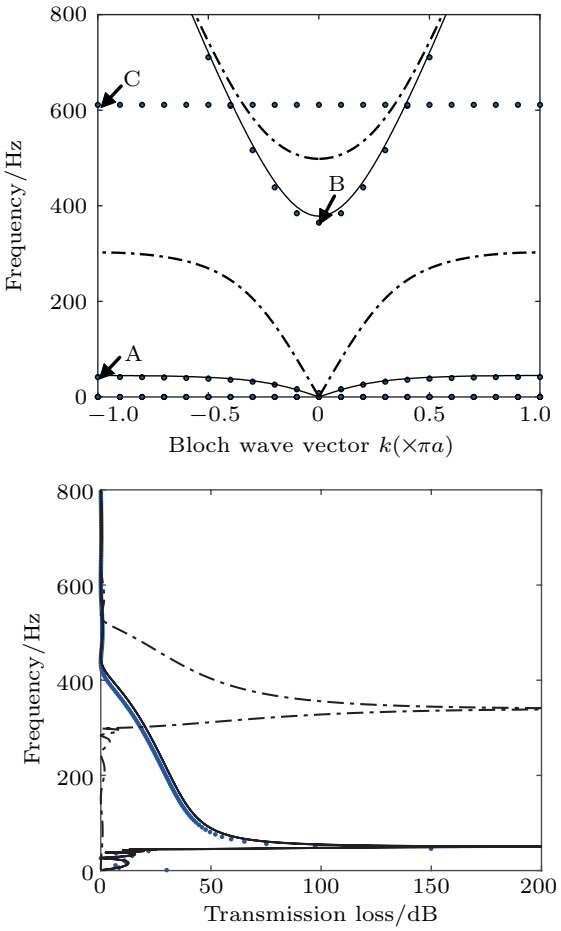


Fig. 7. Band structure and STL with $M = 1$. Solid and dotted lines correspond to the TMM and FEM results for elastic HR, and the dash dot lines correspond to rigid HR results calculated by TMM.

The band structure and STL for various values of the number of HRs, M, in one cell are calculated, and the results are shown in Fig. 10. The solid lines, dash dot lines, and dotted lines correspond to $M = 1$, 2, and 4, respectively. We find that the bandgap range becomes wider. The normalized gap widths are $\Delta f/f_{\rm g} = 1.57$, 1.70, and 1.80 for $M = 1$, 2, and 4, respectively. Additionally, the STL becomes stronger as M increases. Therefore, a low-frequency, broadband and strong attenuation bandgap with a small sized HR is obtained.

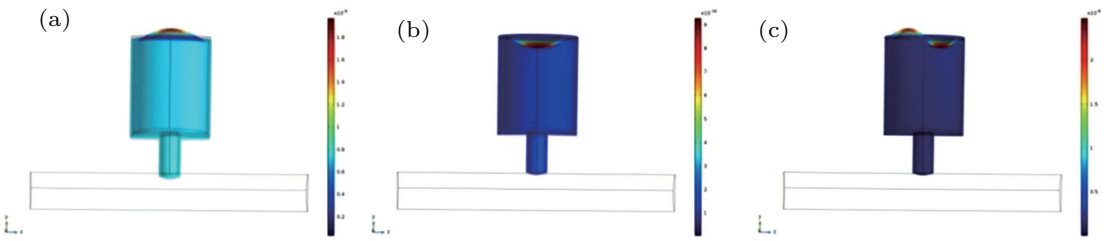


Fig. 8. (color online) Mode shapes of the unit cell for various Bloch wave vectors, corresponding to points A, B, and C in Fig. 7.

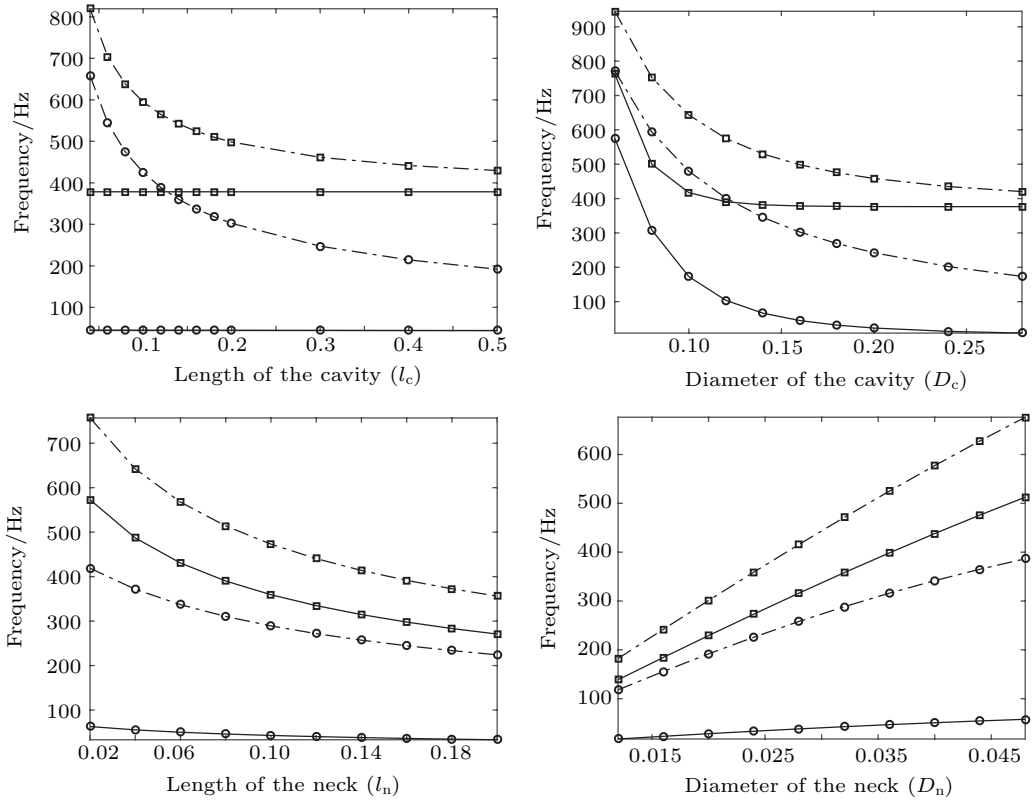


Fig. 9. Effects of the geometric parameters of the HR on band gaps. The continuous and dash-dot lines correspond to an elastic HR and a rigid HR, respectively. The symbol ∘ (□) describes the start (cutoff) frequency.

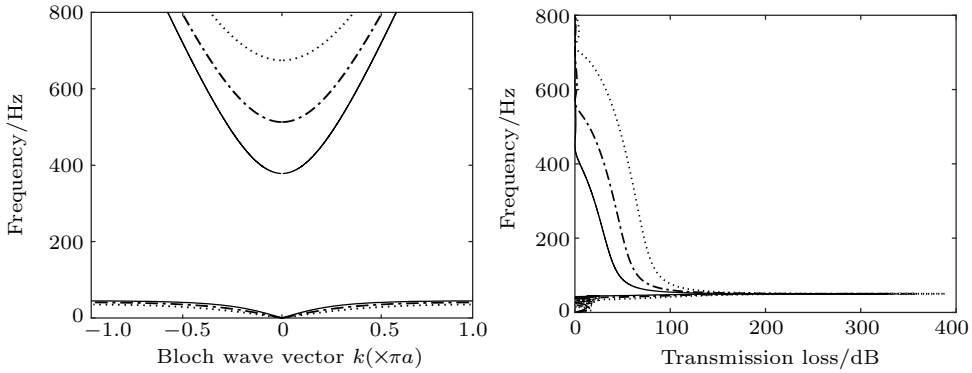


Fig. 10. Band structure and STL for various numbers of HRs. Solid, dash dot, and dotted lines correspond to $M = 1$, 2, and 4, respectively.

5. Negative bulk modulus of periodic with elastic HRs

In the last decade, negative constituent parameters of acoustic metamaterials have been investigated,[21,26–28] which provides new propagation characteristics for acoustic waves.

The one-dimensional (1D) microscope acoustic wave equations in the lossless case can be expressed in the following equation[27,28]

$$\frac{\partial u}{\partial x} = -\frac{1}{K_{\text{eff}}}\dot{p}. \tag{14}$$

If we neglect the harmonic dependence $\mathrm{e}^{\mathrm{i}\omega t}$, then we have

$$\frac{\partial u}{\partial x} = -\frac{\mathrm{i}\omega}{K_{\text{eff}}}p. \tag{15}$$

The propagation of the acoustic wave in the n-th unit can be described by the approximate differential equations[27]

$$\frac{\partial u}{\partial x} = -\frac{Y}{a_{\text{p}}}p, \tag{16}$$

where $Y = 1/Z_{\text{EH}}$ is the admittance of an HR, which is different from that in Ref. [27].

By combining Eqs. (15) and (16), the effective bulk modulus can be obtained as follows:

$$\frac{1}{K_{\text{eff}}} = -\frac{\mathrm{i}}{a_{\text{p}}Z_{\text{EH}}\omega}. \tag{17}$$

The relation between the real part of the $1/K_{\text{eff}}$ and frequency is illustrated in Fig. 11(a). One can find that the effective bulk modulus above the resonant frequency 46 Hz is negative.

Based on Eq. (8), the effective acoustic impedance with M HRs in one cell will be Z_{EH}/M. The solid, dash dot, and dotted lines in Fig. 11(a) correspond to $M = 1$, 2, and 4, respectively. The absolute of the real part of the $1/K_{\mathrm{eff}}$ become larger as M increases. This can explain the causes of broadband and stronger attenuation as M increases. For comparison, the effective bulk modulus for rigid HR is calculated in Fig. 11(b). In this case, the effective bulk modulus above the resonant frequency 340 Hz is negative.

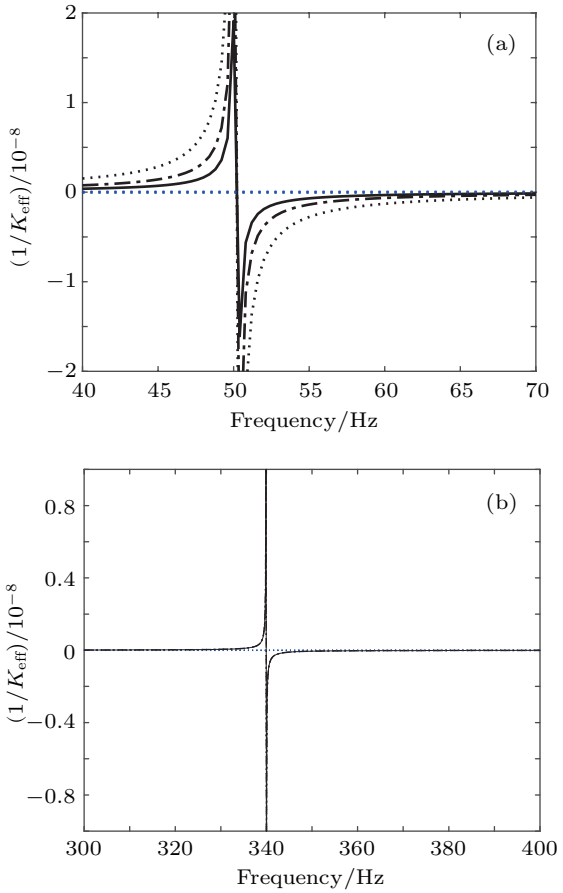


Fig. 11. (a) Effective bulk moduli for elastic HR, where the solid, dash-dot, and dotted lines correspond to $M = 1$, 2, and 4, respectively. (b) Effective bulk modulus for rigid HR.

6. Conclusions

The propagation of acoustic waves in a periodic pipe with elastic Helmholtz resonators has been studied theoretically in this paper.

The TMM is developed to conduct the investigation. The correctness of the TMM is validated by comparing their results with the results from the FEM.

For one unit, the simplified acoustic impedance is obtained with appropriate boundary conditions. The resonance frequency of an elastic HR is much less than that of a rigid HR with the same sized cavity. Additionally, the resonant frequency for an elastic HR depends on the top panel but not the cavity size. The number of HRs in a single cell will increases the STL in the broadband frequency range.

For a periodic pipe, periodic elastic HRs will be beneficial to the generation of a low-frequency and a broadband gap. By calculating the mode shapes, the resonance of the top panel reveals the band gap formation mechanism. For the same sized cavity, the normalized gap width for elastic HRs is 1.57, and the normalized gap width for rigid HRs is 0.49. The start frequency and cutoff frequency are independent of the length of the cavity, and the effects of the geometric parameters of the neck on the start frequency are all trivial.

This work opens a new avenue to controlling low-frequency and broadband noise of a fluid-filled pipe system.

References

[1] Yu D L, Wen J H, Zhao H G, Liu Y Z and Wen X S 2008 *J. Sound Vib.* **318** 193
[2] Li Y F, Shen H J, Zhang L K, Su Y S and Yu D L 2016 *Phys. Lett. A* **380** 2322
[3] Xuan L K, Liu Y, Gong J F, Ming P J and Ruan Z Q 2017 *Adv. Mech. Eng.* **9** 1
[4] Munjal M L 2014 *Acoustics of Ducts and Mufflers* (West Sussex: John Wiley & Sons Ltd.)
[5] Seo S H and Kim Y H 2005 *J. Acoust. Soc. Am.* **118** 2332
[6] Photiadis D M 1991 *J. Acoust. Soc. Am.* **90** 1188
[7] Norris A N and Wickham G 1993 *J. Acoust. Soc. Am.* **93** 617
[8] Wang Z F, Hu Y M, Xiong S D, Luo H, Meng Z and Ni M 2009 *Acta Phys. Sin.* **58** 2507 (in Chinese)
[9] Sang Y J, Lan Y and Ding YW 2016 *Acta Phys. Sin.* **65** 024301 (in Chinese)
[10] Zhou C G, Liu B L, Li X D and Tian J 2007 *Acta Acustica* **32** 426
[11] Cummer S A, Christensen J and Alù A 2016 *Nat. Rev. Mater.* **1** 16001
[12] Hussein M I, Leamy M J and Ruzzene M 2014 *ASME Appl. Mech. Rev.* **66** 040802
[13] Fang X, Wen J H, Bonello B, Yin J F and Yu D L 2017 *Nat. Commun.* **8** 1288
[14] Wei Z D, Li B R, Du J M and Yang G. 2016 *Chin. Phys. Lett.* **33** 044303
[15] Yang Z, Mei J, Yang M, Chan N H and Sheng P 2008 *Physics* **101** 204301
[16] Cai L, Wen J H, Yu D L, Lu Z M and Wen X S 2014 *Chin. Phys. Lett.* **31** 094303
[17] Zhao H G, Liu Y Z, Wen J H, Yu D L, Wang G and Wen X S 2006 *Chin. Phys. Lett.* **23** 2132
[18] Sun H W, Lin G C, Du X W and Pai P F 2012 *Acta Phys. Sin.* **61** 154302 (in Chinese)
[19] Amireddy K K, Amaniam K B and Rajagopal P 2017 *Sci. Rep.* **7** 7777
[20] Cheer J, Daley S and McCormick C 2017 *Smart Mater. Struct.* **26** 025032
[21] Xia B Z, Qin Y, Chen N, Yu D J and Jiang C 2017 *Sci. China-Tech. Sci.* **60** 385
[22] Farooqui M, Elnady T and Akl W 2016 *J. Acoust. Soc. Am.* **139** 3277
[23] Ji Z L 2015 *Acoustic theory and design of muffler* (Beijing: Science Press)
[24] Zhang H, Xiao Y, Wen J H, Yu D L and Wen X S 2016 *Appl. Phys. Lett.* **108** 141902
[25] Yu D L, Du C Y, Shen H J, Liu J W and Wen J H 2017 *Chin. Phys. Lett.* **34** 076202
[26] Lee S H and Wright O B 2016 *Phys. Rev. B* **93** 24302
[27] Cheng Y, Xu J Y and Liu X J 2008 *Phys. Rev. B* **77** 045134
[28] Li Y F, Lan J, Li B S, Liu X Z and Zhang J S 2016 *J. Appl. Phys.* **120** 145105